Molecular Therapy
Nucleic Acids
Original Article

miR-7 Suppresses Tumor Progression by Directly Targeting MAP3K9 in Pancreatic Cancer

Jun Xia,[1,5] Tong Cao,[2,5] Cong Ma,[2,5] Ying Shi,[1] Yu Sun,[1] Z. Peter Wang,[1,3,4] and Jia Ma[1]

[1]Department of Biochemistry and Molecular Biology, School of Laboratory Medicine, Bengbu Medical College, Anhui 233030, China; [2]Research Center of Clinical Laboratory Science, Bengbu Medical College, Anhui 233030, China; [3]Center of Scientific Research, The Second Affiliated Hospital of Wenzhou Medical University, Wenzhou, Zhejiang 325027, China; [4]Department of Pathology, Beth Israel Deaconess Medical Center, Harvard Medical School, Boston, MA, USA

Extensive research has suggested that miR-7 plays a critical role in cancer progression. However, the biological function of miR-7 in pancreatic cancer (PC) progression is poorly understood. Therefore, in the present study, we investigated the function of miR-7 and its molecular mechanism in PC progression. We used multiple methods, such as MTT, FACS, Transwell assay, RT-PCR, western blotting, and transfection to investigate the role of miR-7 in PC cells. We found that miR-7 suppressed cell growth, migration, and invasion but induced apoptosis in PC cells. Moreover, overexpression of miR-7 repressed tumor growth in mice, suggesting that miR-7 could exert its tumor-suppressive function in PC. Mechanistically, we validated that MAP3K9 is a direct target of miR-7, which significantly enhanced PC cell proliferation and inhibited cell apoptosis partly through activation of the MEK/ERK pathway and NF-κB pathway. Moreover, rescue experiments also showed that miR-7 suppressed PC cell proliferation and induced PC cell apoptosis by directly targeting MAP3K9, leading to inhibition of the MEK/ERK and NF-κB pathways. Taken together, these results suggest that miR-7/MAP3K9 is critically involved in PC progression and that miR-7 may be a potential target for PC treatment.

INTRODUCTION

The incidence of pancreatic cancer (PC) has increased globally in the past decades.[1–3] About 55,440 new cases of PC are estimated in the USA in 2018, including 29,200 new cases in males and 26,240 female patients.[4] As a highly fatal malignance, PC has the lowest survival of human cancers; the 5-year relative survival rate only reaches 8%.[4] Thus, it is pivotal to clarify the underlying molecular mechanism of pancreatic carcinogenesis and to find novel treatments for PC.

Extensive research in recent years has indicated that miR-7 plays an important role in cancer progression. Studies have demonstrated that miR-7 functions as a tumor suppressor in cancer development and progression. For example, miR-7 suppresses cell growth and induces cell apoptosis by targeting oncogenic Yin Yang 1 (YY1) in colorectal cancer.[5] Moreover, corticotropin-releasing hormone receptor 2 and urocortin-2 (CRHR2/Ucn2) signaling is involved in negative regulation of the miR-7/YY1/Fas circuitry to increase the sensitivity of colorectal cancer cells to Fas- and FasL-mediated apoptosis.[6] In addition, downregulated expression of miR-7 was observed in glioma samples and correlated with tumor grades.[7,8] Furthermore, the methylation status of miR-7 is associated with upregulation of MAF bZIP transcription factor G (MAFG), leading to CDDP (cisplatin) resistance and a worse prognosis in ovarian cancer patients.[9] Suppression of tumor metastasis by miR-7 was also found to be due to epidermal growth factor receptor (EGFR) inhibition and AKT/ERK (extracellular signal-regulated kinase) inactivation in ovarian cancer cells.[10] However, miR-7 has been classified as an oncogene in some types of human cancers. For instance, serum miR-7 expression was obviously higher in epithelial ovarian cancer patients than in healthy control, which correlates with lymph node metastases and Federation of Gynecology and Obstetrics (FIGO) stages III–IV.[11] Consistently, ectopic expression of miR-7 strengthened the migration and invasion capacities of ovarian cells,[11] indicating that miR-7 could exert its anti-tumor activity in ovarian cancer. Hence, the function of miR-7 in human cancers has not been clearly elucidated and should be intensively investigated.

MLKs (mixed-lineage kinases) were identified as a family of serine/threonine protein kinases that serve upstream of MAPKs (mitogen-activated protein kinases) to activate the JNK (Jun N-terminal kinase) pathway, p38 MAPKs,[12] and the MEK (MAPK kinase)/ERK pathway.[13] Some evidence shows that MLKs such as MLK3 and MLK4 may contribute to an oncogenic role in several human cancers.[14,15] MLK1, also named MAP3K9 (mitogen-activated protein kinase kinase kinase 9), has been classified as an oncoprotein.[16] Specifically, inhibition of MAP3K9 retarded PC cell necroptosis induced by the second mitochondrial activator of caspases (Smac) mimetic BV6.[16] Recently, miR-148a[17] and miR-34a[18] exerted their tumor suppressor functions via inhibition of MAP3K9 in cutaneous squamous cell carcinoma and neroblastoma, respectively. Although these

Received 13 June 2018; accepted 16 August 2018;
https://doi.org/10.1016/j.omtn.2018.08.012.

[5]These authors contributed equally to this work.

Correspondence: Z. Peter Wang, Department of Pathology, Beth Israel Deaconess Medical Center, Harvard Medical School, Boston, MA, USA.
E-mail: zwang6@bidmc.harvard.edu
Correspondence: Jia Ma, Department of Biochemistry and Molecular Biology, School of Laboratory Medicine, Bengbu Medical College, Anhui 233030, China.
E-mail: majiamj10@126.com

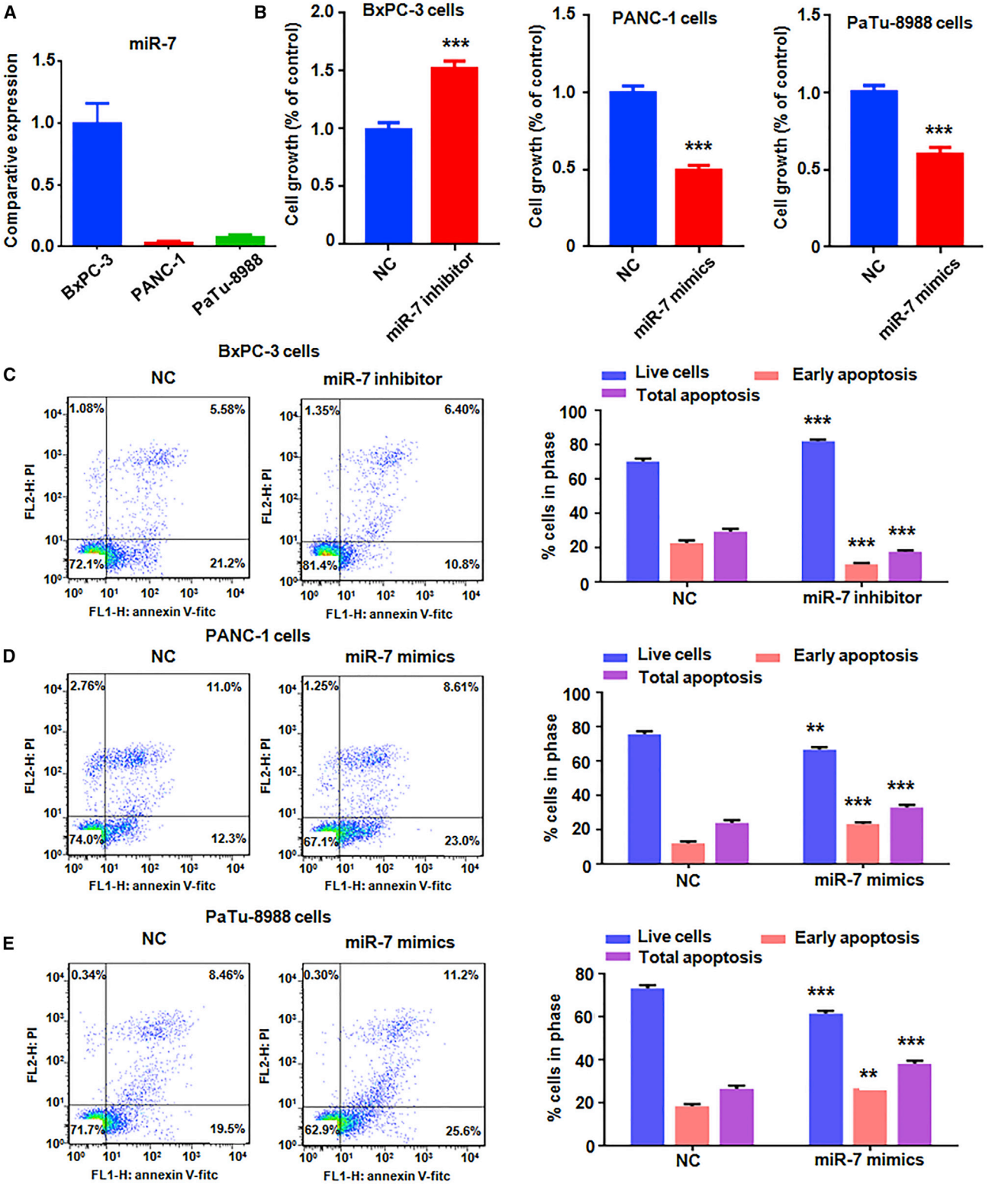

(legend on next page)

reports have shown the function of MAP3K9 in cancer, the molecular mechanism of MAP3K9-mediated tumor progression is poorly understood, and extensive research is necessary to explore the molecular basis of MAP3K9 in PC.

In the present study, we investigated the biological functions of miR-7 in PC *in vitro* and *in vivo*. We also validated whether miR-7 directly targeted MAP3K9 to inhibit PC progression. We found that miR-7 exhibited a tumor-suppressive function by directly targeting MAP3K9 in PC cells. Moreover, we found that MAP3K9 enhanced cell growth partly through regulation of its downstream pathways, the MEK/ERK and NF-κB (nuclear factor κB) pathways. Our results revealed that the miR-7/MAP3K9 axis might play a pivotal role in PC progression.

RESULTS

Overexpression of miR-7 Suppresses Cell Proliferation and Induces Cell Apoptosis

To dissect the biological function of miR-7, we planned to upregulate or downregulate the expression of miR-7 in PC cells and then measure the cellular progression after miR-7 changes. We first assessed the basal levels of miR-7 expression by real-time RT-PCR in different PC cell lines. Our results showed that BxPC-3 cells exhibited the highest expression of miR-7, whereas PANC-1 and PaTu-8988 cells had lower expression of miR-7 (Figure 1A). Thus, miR-7 inhibitors were transfected into BxPC-3 cells to reduce miR-7 expression, whereas miR-7 mimics were transfected into PANC-1 and PaTu-8988 cells to augment miR-7 expression for the subsequently assays. We found that miR-7 inhibitors significantly reduced the miR-7 level in BxPC-3 cells and that miR-7 mimic treatment increased the expression of miR-7 in PANC-1 and PaTu-8988 cells (Figure S1A).

To ascertain whether cell proliferation is regulated by miR-7, we performed an MTT (3-4,5-dimethylthiazol-2,5-diphenyltetrazolium bromide) assay in PC cells after miR-7 changes. Our MTT assay results showed that miR-7 inhibitors increased the cell proliferation of BxPC-3 cells, whereas miR-7 mimic transfection decreased the cell proliferation of PANC-1 and PaTu-8988 cells (Figure 1B). Next, cell apoptosis was measured in PC cells after miR-7 modification. We observed that apoptosis was induced by miR-7 mimic transfection in PANC-1 and PaTu-8988 cells but inhibited by miR-7 inhibitor transfection in BxPC-3 cells (Figures 1C–1E). Specifically, miR-7 inhibitors significantly decreased the percentage of apoptosis cells, including early apoptosis cells and total apoptosis cells, for BxPC-3 cells (Figure 1C). However, miR-7 mimics obviously increased early apoptosis cells and total apoptosis cells for PANC-1 and PaTu-8988 cells (Figures 1D and 1E).

Overexpression of miR-7 Suppresses Cell Migration and Invasion

To characterize whether miR-7 could influence cell migration, we conducted a wound healing assay in PC cells after miR-7 modification. From the wound healing assay results, we saw that miR-7 inhibitors promoted cell migration in BxPC-3 cells, but miR-7 mimics retarded cell migration in PANC-1 and PaTu-8988 cells (Figure 2A). A transwell assay was applied for measuring cell migration and invasion in PC cells after miR-7 changes. We found that miR-7 inhibitors boosted the migration and invasion capacity in BxPC-3 cells, whereas miR-7 mimics exerted the opposite effects on cell migration and invasion capacity (Figures 2B and 2C; Figure S1B). These results reveal that miR-7 retards cell migration and invasion in PC cells.

miR-7 Overexpression Represses Tumor Growth *In Vivo*

To further elucidate the role of miR-7 *in vivo*, we investigated the effect of miR-7 ectopic expression on the growth of PC xenografts in nude mice. Stable overexpression of pre-miR-7 caused remarkably inhibition effects on tumor growth compared with the control group (Figure 2D). The tumor sizes and tumor weights were obviously less in the pre-miR-7 group compared with the control group (Figures 2E and 2F). We further examined miR-7 expression in tumor masses after the mice were sacrificed and the tumors were harvested. The results showed remarkably higher expression of miR-7 in the stable overexpression pre-miR-7 group (Figure 2G). This finding indicates that overexpression of miR-7 inhibits tumor growth in mice.

MAP3K9 Is a Direct Target of miR-7

To screen out a direct target of miR-7, different miRNA target prediction tools were employed. MAP3K9 was identified as a target of miR-7 by 5 prediction tools, including miRTAR, miRDB, TargetScan, miRanda, and DIANA (Figure 3A). Only one binding site was predicted between the MAP3K9 3′ UTR sequence and the conserved seed sequence of miR-7 by TargetScan and miRDB (Figure 3B). We constructed the wild-type pmirGLO-MAP3K9-3′ UTR vector and the mutant-type pmirGLO-MAP3K9-mut-3′ UTR vector (containing 4 base mutations in the miR-7 binding sites) for our study (Figure 3B).

MAP3K9 mRNA and protein levels were detected in PC cells with transfection of miR-7 mimics or miR-7 inhibitors. miR-7 mimics decreased MAP3K9 mRNA and protein expression in PANC-1 and PaTu-8988 cells, whereas miR-7 inhibitors increased MAP3K9 expression in BxPC-3 cells (Figures 3C–3E). Consistent with these results, MAP3K9 protein expression, measured by western blotting, was also remarkably reduced in PANC-1 xenografts with ectopic expression of pre-miR-7 (Figure 3F).

Figure 1. miR-7 Inhibited Cell Proliferation and Induced Cell Apoptosis in PC Cells

(A) The comparative expression of miR-7 was measured by real-time RT-PCR in PC cells. (B) An MTT assay was performed after miR-7 inhibitor treatment in BxPC-3 cells or miR-7 mimic treatment in PANC-1 cells and PaTu-8988 cells for 72 hr. Error bar: SE. ***$p < 0.001$ versus control. (C) Cell apoptosis was measured after miR-7 inhibitor treatment for 48 hr in BxPC-3 cells. Error bar: SE. ***$p < 0.001$ versus control. (D) Cell apoptosis was detected after miR-7 mimic treatment for 48 hr in PANC-1 cells. Error bar: SE. **$p < 0.01$ versus control; ***$p < 0.001$ versus control. (E) Cell apoptosis was determined after miR-7 mimic treatment for 48 hr in PaTu-8988 cells. Error bar: SE. **$p < 0.05$ versus control; ***$p < 0.001$ versus control.

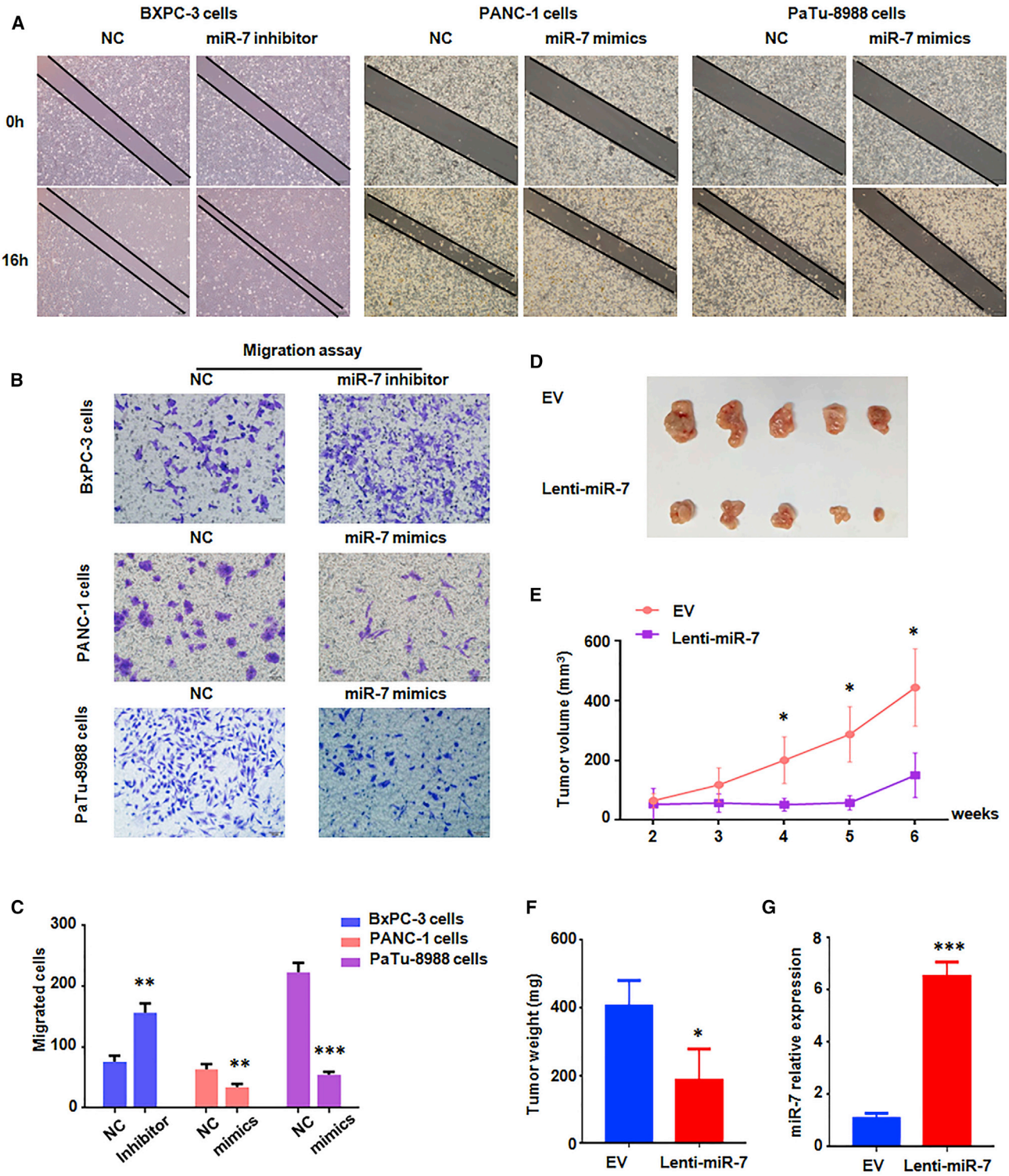

Figure 2. miR-7 Inhibited Cell Migration in PC Cells and Repressed Tumor Growth *In Vivo*

(A) Wound healing assays were performed after miR-7 inhibitor treatment in BxPC-3 cells or miR-7 mimic treatment in PANC-1 cells and PaTu-8988 cells for 16 hr. NC, negative control. (B) Transwell migration assays were conducted after miR-7 inhibitor treatment in BxPC-3 cells or miR-7 mimic treatment in PANC-1 cells and PaTu-8988

(legend continued on next page)

To evaluate the direct binding interaction between miR-7 and the MAP3K9 3′ UTR, a dual luciferase reporter assay was used in 293T cells. miR-7 mimics dramatically reduced luciferase activity in the wild-type MAP3K9 3′ UTR group. However, the suppression effects on the luciferase reporter activity were not observed in the mutant-type MAP3K9 3′ UTR group (Figure 3G). All results imply that MAP3K9 is a direct target of miR-7.

MAP3K9 Promotes Cell Proliferation and Inhibits Apoptosis Partly through Activation of the MEK/ERK Pathway and the NF-κB Pathway

Because miR-7 exerted tumor suppression effects and negatively regulated MAP3K9 expression in PC, we subsequently took an interest in exploring the oncogenic roles of MAP3K9 in PC. Both the ectopic expression and small interfering RNA (siRNA)-generated knockdown of MAP3K9 were used in BxPC-3 cells, PANC-1 cells, and PaTu-8988 cells, respectively, for our following study. A western blot assay was performed to evaluate the knockdown efficacy of MAP3K9 siRNA and showed that MAP3K9 siRNAs inhibit the expression of MAP3K9 in PANC-1 cell lines (Figure S1C). The MAP3K9-Homo-853 siRNA sequence exhibiting the highest knockdown efficacy was selected for subsequent studies. Moreover, our qRT-PCR and western blot results demonstrated that MAP3K9 cDNA transfection increased its expression in BxPC-3 cells, whereas MAP3K9 siRNA transfection decreased the level of MAP3K9 in PANC-1 and PaTu-8988 cells (Figures 4A–4C).

Because MAP3K9 is a member of the MAPKKK (MAPK kinase kinase) family, we further explored the association between MAP3K9 expression with MAPK and NF-κB signaling. As shown in Figures 4B and 4C, MAP3K9 overexpression caused upregulated expression of pMEK1/2, pERK1/2, and NF-κB in BxPC-3 cells, paralleled by downregulated expression of pMEK1/2, pERK1/2, and NF-κB after MAP3K9 siRNA treatment in PANC-1 and PaTu-8988 cells. These finding indicate that MAP3K9 governs its downstream targets, the MEK/ERK signaling pathway and the NF-κB signaling pathway.

The results of the MTT assay showed that upregulation of MAP3K9 promoted cell proliferation in BxPC-3 cells, whereas downregulation of MAP3K9 inhibited cell growth in PANC-1 cells and PaTu-8988 cells (Figure 5A). From the apoptosis assay by Annexin V-fluorescein isothiocyanate (FITC) and PI staining, MAP3K9 overexpression led to a decreased percentage of apoptotic cells for BxPC-3 cells; on the contrary, MAP3K9 knockdown caused an increased percentage of apoptotic cells (Figures 5B–5D). In summary, the results reveal that MAP3K9 exerts its tumorigenic effect on cell growth and apoptosis in PC cells.

MAP3K9 Overexpression Rescues miR-7-Mediated Cell Growth Inhibition and Apoptosis Induction

Rescue experiments were also performed to confirm whether miR-7 exerts its tumor-suppressive effect via inhibition of MAP3K9 in PC cells. MAP3K9 knockdown diminished the cell growth-promoting effects of miR-7 downregulation in BxPC-3 cells (Figure 6A). Re-expression of MAP3K9 neutralized the growth inhibition effects of miR-7 overexpression in PANC-1 cells and PaTu-8988 cells (Figure 6A). Consistently, MAP3K9 re-expression weakened the apoptosis induction effects of miR-7 mimics in PANC-1 and PaTu-8988 cells, whereas MAP3K9 siRNA attenuated the cell apoptosis inhibition effects of miR-7 inhibitors in BxPC-3 cells (Figures 6B–6D). More importantly, re-expression of MAP3K9 partially restored the downregulated protein expression of pMEK1/2, pERK1/2, and NF-κB by miR-7 overexpression in PANC-1 and PaTu-8988 cells (Figure 6E). These results suggest that miR-7 suppresses cell proliferation and induces cell apoptosis partially by targeting MAP3K9.

DISCUSSION

In recent years, some studies have demonstrated that miR-7 fulfills the antitumor function in pancreatic tumorigenesis.[19,20] In line with this, miR-7 suppresses PC proliferation and mobility because of repressing autophagy to reduce the glucose provision to glycolysis metabolism through upregulation of LKB1-AMPK (AMP-activated protein kinase)-mTOR (mammalian target of rapamycin) signaling.[20] A similar report has shown that miR-7 contributes a positive role of suppressing PC progression through downregulation of the interleukin-2 (IL-2) oncoprotein in PC.[21] However, an opposite view has been suggested; namely, that the expression of miR-7 is increased by the activation of MAPK signaling in PC cells,[22] according to higher expression of MAPK-associated miR-7 in serum in PC patients compared with autoimmune pancreatitis.[23] These reports suggest that the function of miR-7 in the progression of PC and its underlying mechanism remain to be extensively elucidated. According to our present study, miR-7 significantly suppressed PC cell growth and mobility and induced cell apoptosis *in vitro*. In support of these findings, overexpression of miR-7 retarded tumor growth in the PC xenograft model. Our results revealed that miR-7 functions as a tumor suppressor in PC, suggesting that miR-7 might be a potential target for PC treatment.

Impressively, we found that miR-7 directly targeted MAP3K9, leading to regulation of MAP3K9 downstream genes in PC cells. It has been reported that MAP3K9 mutations can be observed in different human cancers, including salivary gland malignancy,[24] lung cancer,[25] colon cancer,[26] and metastatic melanoma.[27] Gain-of-function mutations in MAP3K9 have been founded in lung cancer samples, and depletion of mutated MAP3K9 suppresses cell proliferation and generates

cells for 24 hr. (C) Quantitative results are illustrated for the transwell migration assays. Error bar: SE. **$p < 0.01$ versus control; ***$p < 0.001$ versus control. (D) Overexpression of miR-7 repressed tumor growth in mice. Nude mice were inoculated with lentivirus-transduced PANC-1 cells with empty vector (EV) or stably overexpressed pre-miR-7 and sacrificed 6 weeks after inoculation. (E) The volume of tumors was measured in mice. Error bar: SE. *$p < 0.01$ versus control. (F) Tumor weights were measured in mice. Error bar: SE. *$p < 0.01$ versus control. (G) A real-time RT-PCR assay was used to measure miR-7 in mouse tumor masses. Error bar: SE. ***$p < 0.001$ versus control.

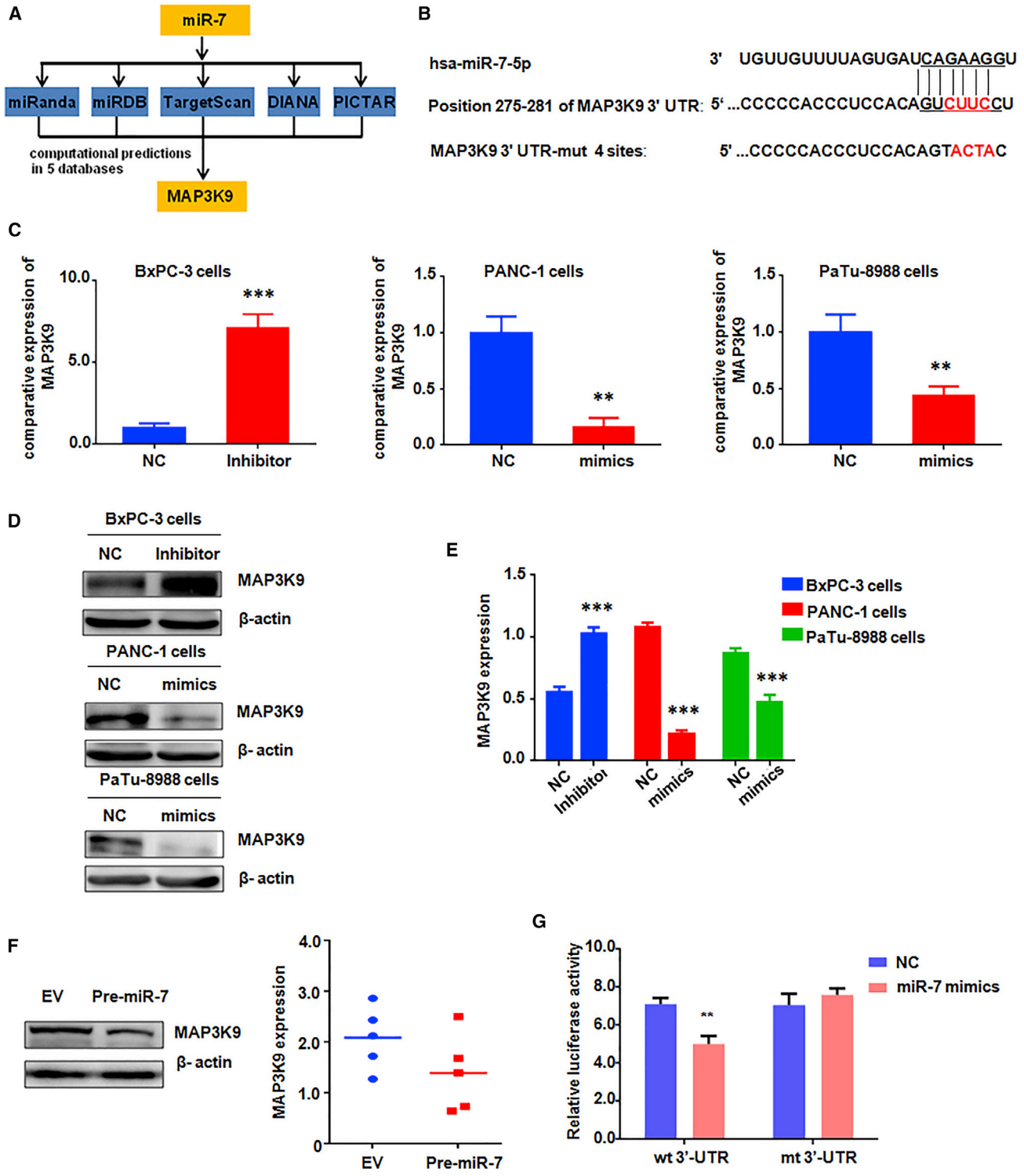

Figure 3. MAP3K9 Is a Target of miR-7

(A) Five public algorithms, including TargetScan, PicTar, miRDB, TargetScan, and miRanda, were used to predict that MAP3K9 might be a potential target of miR-7. (B) The direct physical interaction between miR-7 and the MAP3K9 3′ UTR and mutation of the putative miR-7-binding site on the MAP3K9 3′ UTR. (C) A real-time RT-PCR assay was performed to detect the mRNA level of MAP3K9 after miR-7 inhibitor treatment in BxPC-3 cells or miR-7 mimic treatment in PANC-1 cells and PaTu-8988 cells. Error bar: SE.

(legend continued on next page)

specific killing of lung cancer cells.[25] However, MAP3K9 mutations in its kinase domain have been proposed to inhibit its kinase activity and the phosphorylation level of downstream MAP kinases, and MAP3K9 siRNA leads to chemoresistance in melanoma cells,[27] which suggests that MAP3K9 may play contrary roles in lung cancer and melanoma. Moreover, it has been reported that MAP3K9 knockout has no effects on mouse phenotype, suggesting that MAP3K9 is not essential for survival in mice.[28] These conflicting results show that the carcinogenic role of MAP3K9 needs to be studied further. To explore the role of MAP3K9 in PC, we investigated the function of MAP3K9 in cell growth and apoptosis in PC cells. Our results suggest that MAP3K9 plays an oncogenic role in PC.

Furthermore, MLKs have been reported to phosphorylate MEK and activate the MEK/ERK pathway.[13] Consistently, miR-7 has been suggested to inactivate ERK1/2 by downregulating EGFR to inhibit cell metastasis in ovarian cancer.[10] These results imply that miR-7 might target the MAP3K9/MEK/ERK pathway, leading to suppression of cell proliferation and induction of cell apoptosis in PC cells. The MEK/ERK pathway is a canonical pathway of carcinogenesis drivers[29–31] and shows cross-talk with the NF-κB pathway.[32] As shown in our results, MAP3K9 activates the MEK/ERK and NF-κB pathways, and miR-7 inhibits PC cell growth by directly targeting MAP3K9, subsequently leading to inactive MEK/ERK and NF-κB pathways. As described in our previous study, curcumin depresses cell growth and mobility through upregulation of miR-7 in PC.[33] However, whether curcumin suppresses PC progression partly through upregulation of miR-7 and downregulation of MAP3K9 and MEK/ERK needs to be investigated. In summary, our results provide a novel mechanism of miR-7-mediated suppressive effects on PC tumorigenesis. This study also indicates that restoration of miR-7 expression and inhibition of MAP3K9 expression might be potential strategies for PC treatment.

MATERIALS AND METHODS

Cell Lines and Cell Culture

Human PC cells, including BxPC-3, PANC-1, and Patu-8988 cells, and HEK293T cells were obtained from American Type Culture Collection (Manassas, VA, USA). These cells were cultured in DMEM (Gibco, New York, USA) with 10% fetal bovine serum and maintained in a water-jacketed incubator at 37°C with 5% CO_2. PANC-1 cells were infected with a lentivirus encoding precursor miR-7 or an empty vector and selected with puromycin for 2 weeks to establish stable miR-7-expressing cells.

Transfection of Oligonucleotide Sequences and Plasmids

Transfection of oligonucleotide sequences and plasmids was conducted using Lipofectamine 2000 reagent (Invitrogen, Carlsbad, CA, USA) following the manufacturer's instructions. miR-7 mimic sequences were designed to be the same as the mature miR-7 sequences as follows: 5′-TCG AAG ACT AGT GAT TTT GTT GT-3′. miR-7 inhibitor sequences were complementary to mature miR-7 sequences as follows: 5′-ACA ACA AAA TCA CTA GTC TTC CA-3′. The MAP3K9 siRNA sequences were designed as follows: MAP3K9-Homo-1403, 5′-GUC CCU GGU AGA UGG AUA UTT-3′ (sense) and 5′-AUA UCC AUC UAC CAG GGA CTT-3′ (antisense); MAP3K9-Homo-853, 5′-GGG AGC UGA ACA UCA UCA UTT-3′ (sense) and 5′-AUG AUG AUG UUG AGC UCC CTT-3′ (antisense); MAP3K9-Homo-2080, 5′-CCG ACA GCG AUG AAA UUG UTT-3′ (sense) and 5′-ACA AUU UCA UCG CUG UCG GTT-3′ (antisense). All oligodeoxynucleotides mentioned above were purchased from Shanghai GenePharma in China.

The precursor miR-7 sequence was synthesized and subcloned into the lentiviral pCDH-CMV-GFP vector by GENEWIZ (Suzhow, China). The retroviral vector pMIGR-MAP3K9 was subcloned from pDONR221 MAP3K9, which was purchased from Addgene. The MAP3K9 3′ UTR sequence was amplified by PCR and subcloned into the pmirGLO vector (Promega, WI, USA). The MAP3K9 3′ UTR mutation vector was constructed by PCR-directed mutagenesis.

RNA Extraction and Real-Time RT-PCR

Total RNA extraction and reverse transcription into cDNA have been described before.[34] miR-7 expression detection was performed using the TaqMan miRNA assay kit (Applied Biosystems, USA), and U6 was used as a reference gene. The MAP3K9 mRNA level was determined using the SYBR Green real-time PCR kit (Takara, Dalian, China), and GAPDH (glyceraldehyde 3-phosphate dehydrogenase) was used as a control for normalization. The primers used for qPCR were as follows: MAP3K9, 5′-GAG TGC GGC AGG GAC GTA T-3′ (sense) and 5′-CCC CAT AGC TCC ACA CAT CAC-3′ (antisense); GAPDH, 5′-GGT GAA GGT CGG AGT CAA CG-3′ (sense) and 5′-TGG GTG GAA TCA TAT TGG AAC A-3′ (antisense).

Western Blotting

Total protein was extracted using cold radioimmunoprecipitation assay (RIPA) buffer with proteinase inhibitors and phosphatase inhibitors. The protein was quantified by BCA assay kit (Beyotime Biotechnology, Beijing, China), separated on SDS-PAGE, and transferred to polyvinylidene fluoride (PVDF) membranes. Then, the PVDF membranes were incubated with the indicated antibodies as follows: MAP3K9 (Abcam), MEK1/2 (Abcam), pMEK1/2 (Abcam), ERK1/2 (Cell Signaling Technology), pERK1/2 (CST), NF-κB (p65, CST), and β-actin (Santa Cruz Biotechnology).

MTT Assay

PC cells were seeded in 6-well plates overnight and transfected with miR-7 mimics or inhibitors and MAP3K9 cDNA or siRNA for

**p < 0.01 versus control, ***p < 0.001 versus control. (D) Western blot analysis was conducted to measure the expression of MAP3K9 after miR-7 inhibitor treatment in BxPC-3 cells or miR-7 mimic treatment in PANC-1 cells and PaTu-8988 cells. (E) Quantitative results for (C). Error bar: SE. ***p < 0.001 versus control. (F) Left: western blot analysis was performed to measure the expression of MAP3K9 in mouse tumors masses. Right: quantitative results for expression of MAP3K9 in mouse tumor masses. (G) Luciferase reporter assays were performed to identify the binding of miR-7 to the MAP3K9 3′ UTR. WT, wild-type; Mut, mutation. Error bar: SE. ***p < 0.01 versus control.

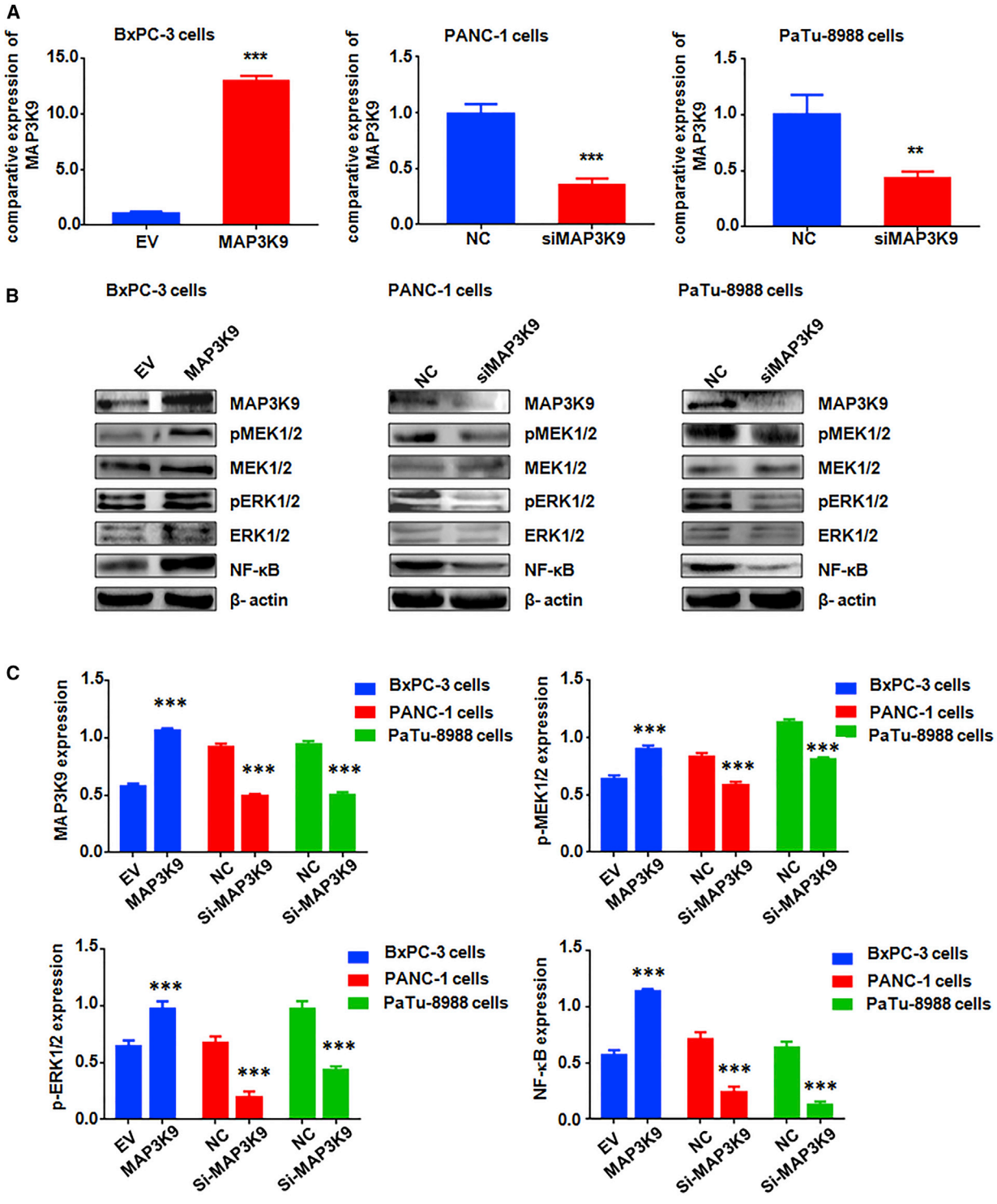

Figure 4. MAP3K9 Expression Associated with MAPK and NF-κB Signaling

(A) A real-time RT-PCR assay was performed to detect the mRNA level of MAP3K9 after transfection with MAP3K9 cDNA in BxPC-3 cells or transfection with MAP3K9 siRNA in PANC-1 cells and PaTu-8988 cells. Error bar: SE. **$p < 0.05$ versus control; ***$p < 0.001$ versus control. (B) Western blot analysis was conducted to measure the expression of MAP3K9, p-MEK1/2, p-ERK1/2, and NF-κB after miR-7 inhibitor treatment in BxPC-3 cells or miR-7 mimic treatment in PANC-1 cells and PaTu-8988 cells. (C) Quantitative results for the western blot analysis in (B). Error bar: SE. ***$p < 0.001$ versus control.

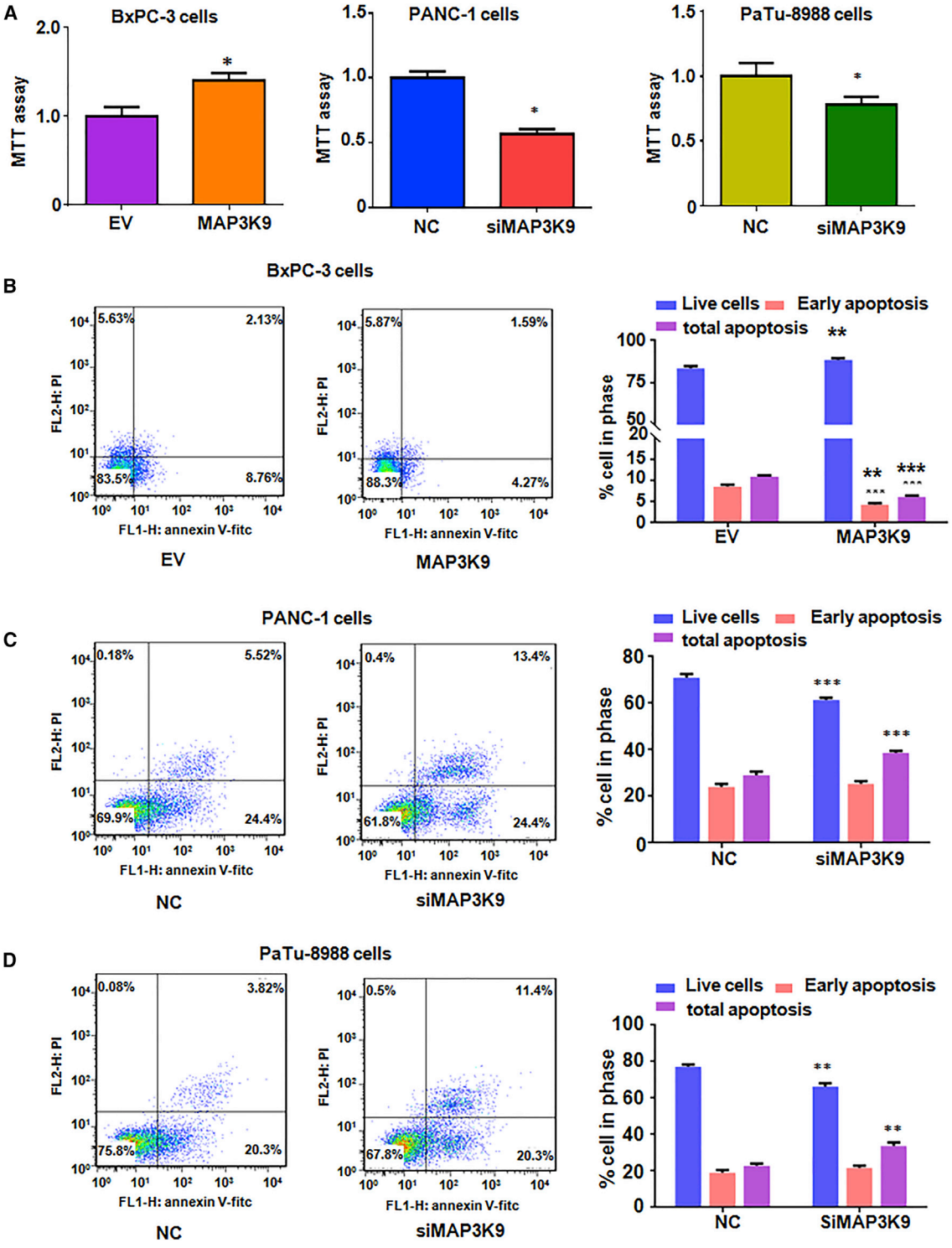

Figure 5. MAP3K9 Promoted Cell Proliferation and Inhibited Cell Apoptosis in PC Cells

(A) An MTT assay was performed after transfection with MAP3K9 cDNA in BxPC-3 cells or transfection with MAP3K9 siRNA in PANC-1 cells and PaTu-8988 cells. Error bar: SE. *$p < 0.05$ versus control. (B) Apoptosis was measured in BxPC-3 cells after MAP3K9 overexpression. Error bar: SE. **$p < 0.01$; ***$p < 0.001$ versus control. (C) Apoptosis was measured in PANC-1 cells after MAP3K9 knockdown. Error bar: SE. ***$p < 0.001$ versus control. (D) Apoptosis was measured in PaTu-8988 cells after MAP3K9 knockdown. Error bar: SE. **$p < 0.01$ versus control.

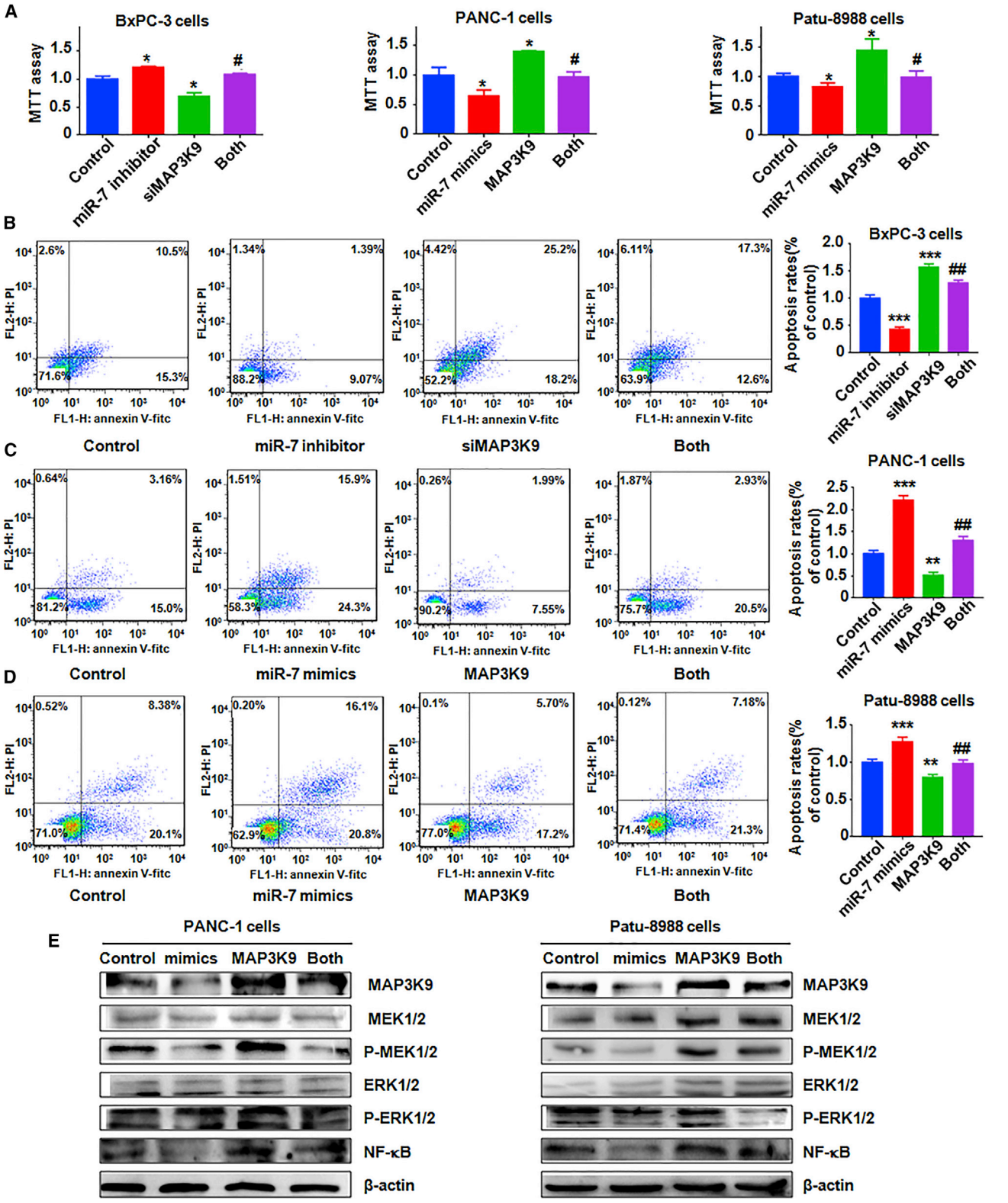

(legend on next page)

48 hr. Then, PC cells were trypsinized and seeded in 96-well plates for 72 hr. Cell viability was detected by MTT assay as described previously.[34]

Cell Apoptosis Assay

PC cells were treated with different transfections as mentioned above. Then, the cells were collected and subjected to Annexin V-FITC/propidium iodide (PI) staining following the manufacturer's instructions. Cell apoptosis was analyzed by flow cytometry as described previously.[35]

Wound Healing Assay

PC cells, after transfection treatment as mentioned above, were seeded in 6-well plates and incubated overnight until the cells achieved 95% confluency. The scratch wound was obtained by scratching the surface cells of plates with a pipette tip, and the detached cells were washed off with PBS. Then the remaining attached cells in 6-well plates were incubated for 16 hr. The wound healing in each well at 0 hr and 16 hr was photographed.

Transwell Migration and Invasion Assay

Cell migration and invasion detection was conducted by transwell assay as described before.[35] The cells were seeded into transwell chambers with 8.0-μm pore membranes in 24-well plates (Corning). For the invasion assay, however, the chambers were prepared by coating with a thin layer of Matrigel (BD Biosciences) before the cells were seeded. After incubation for 24 hr, the bottom-surfaced cells of the chamber were stained with Giemsa solution, photographed, and counted under a microscope.

3′ UTR Assay

293T cells were plated in 24-well plates and cultured for 24 hr to reach 90% confluency. The cells were subsequently cotransfected with miR-7 mimics and pmirGLO -MAP3K9 3′ UTR or pmirGLO -MAP3K9 mut-3′ UTR plasmids using Lipofectamine 2000 reagent. Then, a dual-luciferase reporter assay system was used to detect luciferase activities for analyzing the combination of the miR-7 and MAP3K9 3′ UTR sequence.

In Vivo Experiments

The *in vivo* experiments were performed following the previous description.[35] The animal study was approved by Animal Care and Use Committee of Bengbu Medical College. To establish the PC xenografts, 1×10^7 PC cells, including PANC-1 cells with stably overexpressed pre-miR-7 or control cells transduced with an empty vector, were injected into 5-week-old male nude mice. 2 weeks after injection, the size of the tumors was measured with calipers every week. The mice were killed at 6 weeks, and the tumor masses were stripped to measure the weights.

Statistical Analysis

The data were statistically analyzed by Student's t test for comparing two groups and ANOVA for comparing multiple groups using GraphPad Prism 4.0 (GraphPad, La Jolla, CA). $p < 0.05$ was considered statistically significant.

SUPPLEMENTAL INFORMATION

Supplemental Information includes one figure and can be found with this article online at https://doi.org/10.1016/j.omtn.2018.08.012.

AUTHOR CONTRIBUTIONS

J.X. conceived the work, designed and performed the experiments, analyzed the data, and wrote the manuscript. T.C., C.M., and Y.S. designed and performed the experiments and analyzed the data. Y.S. collected animal tissues and analyzed the data. Z.P.W. and J.M. conceived the work, wrote the manuscript, and critically reviewed and supervised the study.

CONFLICTS OF INTEREST

The authors declare no conflicts of interest.

ACKNOWLEDGMENTS

This work was supported by grants from the National Natural Science Foundation of China (NSFC 81572936, 81502126, and 81773186). This work was also supported in part by the Program for Graduate Research of Bengbu Medical College (Byycx1616).

REFERENCES

1. Lin, Q.J., Yang, F., Jin, C., and Fu, D.L. (2015). Current status and progress of pancreatic cancer in China. World J. Gastroenterol. *21*, 7988–8003.

2. Bouvier, A.M., Uhry, Z., Jooste, V., Drouillard, A., Remontet, L., Launoy, G., and Leone, N.; French Network of Cancer Registries (FRANCIM) (2017). Focus on an unusual rise in pancreatic cancer incidence in France. Int. J. Epidemiol. *46*, 1764–1772.

3. Gordon-Dseagu, V.L., Devesa, S.S., Goggins, M., and Stolzenberg-Solomon, R. (2018). Pancreatic cancer incidence trends: evidence from the Surveillance, Epidemiology and End Results (SEER) population-based data. Int. J. Epidemiol. *47*, 427–439.

Figure 6. MAP3K9 Overexpression Rescued miR-7-Mediated Cell Growth Inhibition and Apoptosis Induction

(A) Left: an MTT assay was conducted in BxPC-3 cells after both miR-7 and MAP3K9 knockdown. Both, miR-7 inhibitor plus MAP3K9 siRNA. *$p < 0.05$ versus control; #$p < 0.05$ versus miR-7 knockdown or MAP3K9 knockdown alone. Center and right: an MTT assay was performed in PANC-1 cells and PaTu-8988 cells after both miR-7 and MAP3K9 overexpression. Both, miR-7 mimics plus MAP3K9 cDNA transfection. *$p < 0.05$ versus control; #$p < 0.05$ versus miR-7 overexpression or MAP3K9 overexpression alone. (B) Apoptosis was measured in BxPC-3 cells after both miR-7 and MAP3K9 knockdown. Both, miR-7 inhibitor plus MAP3K9 siRNA. Error bar: SE. ***$p < 0.001$ versus control; ##$p < 0.01$ versus miR-7 knockdown or MAP3K9 knockdown alone. (C) Apoptosis was detected in PANC-1 cells after both miR-7 and MAP3K9 overexpression. Both, miR-7 mimics plus MAP3K9 cDNA transfection. Error bar: SE. **$p < 0.01$ versus control; ***$p < 0.001$ versus control; ##$p < 0.01$ versus miR-7 knockdown or MAP3K9 overexpression alone. (D) Apoptosis was determined in PaTu-8988 cells after both miR-7 and MAP3K9 overexpression. Both, miR-7 mimics plus MAP3K9 cDNA transfection. Error bar: SE. **$p < 0.01$ versus control; ***$p < 0.001$ versus control; ##$p < 0.01$ versus miR-7 knockdown or MAP3K9 overexpression alone. (E) Western blot analysis was conducted to measure the expression of MAP3K9, p-MEK1/2, p-ERK1/2, and NF-κB in PANC-1 and PaTu-8988 cells after both miR-7 and MAP3K9 overexpression. Both, miR-7 mimics plus MAP3K9 cDNA transfection.

4. Siegel, R.L., Miller, K.D., and Jemal, A. (2018). Cancer statistics, 2018. CA Cancer J. Clin. *68*, 7–30.
5. Zhang, N., Li, X., Wu, C.W., Dong, Y., Cai, M., Mok, M.T., Wang, H., Chen, J., Ng, S.S., Chen, M., et al. (2013). microRNA-7 is a novel inhibitor of YY1 contributing to colorectal tumorigenesis. Oncogene *32*, 5078–5088.
6. Pothoulakis, C., Torre-Rojas, M., Duran-Padilla, M.A., Gevorkian, J., Zoras, O., Chrysos, E., Chalkiadakis, G., and Baritaki, S. (2018). CRHR2/Ucn2 signaling is a novel regulator of miR-7/YY1/Fas circuitry contributing to reversal of colorectal cancer cell resistance to Fas-mediated apoptosis. Int. J. Cancer *142*, 334–346.
7. Koshkin, P.A., Chistiakov, D.A., Nikitin, A.G., Konovalov, A.N., Potapov, A.A., Usachev, D.Y., Pitskhelauri, D.I., Kobyakov, G.L., Shishkina, L.V., and Chekhonin, V.P. (2014). Analysis of expression of microRNAs and genes involved in the control of key signaling mechanisms that support or inhibit development of brain tumors of different grades. Clin. Chim. Acta *430*, 55–62.
8. Visani, M., de Biase, D., Marucci, G., Cerasoli, S., Nigrisoli, E., Bacchi Reggiani, M.L., Albani, F., Baruzzi, A., and Pession, A.; PERNO study group (2014). Expression of 19 microRNAs in glioblastoma and comparison with other brain neoplasia of grades I-III. Mol. Oncol. *8*, 417–430.
9. Vera, O., Jimenez, J., Pernia, O., Rodriguez-Antolin, C., Rodriguez, C., Sanchez Cabo, F., Soto, J., Rosas, R., Lopez-Magallon, S., Esteban Rodriguez, I., et al. (2017). DNA Methylation of miR-7 is a Mechanism Involved in Platinum Response through *MAFG* Overexpression in Cancer Cells. Theranostics *7*, 4118–4134.
10. Zhou, X., Hu, Y., Dai, L., Wang, Y., Zhou, J., Wang, W., Di, W., and Qiu, L. (2014). MicroRNA-7 inhibits tumor metastasis and reverses epithelial-mesenchymal transition through AKT/ERK1/2 inactivation by targeting EGFR in epithelial ovarian cancer. PLoS ONE *9*, e96718.
11. Meng, X., Joosse, S.A., Müller, V., Trillsch, F., Milde-Langosch, K., Mahner, S., Geffken, M., Pantel, K., and Schwarzenbach, H. (2015). Diagnostic and prognostic potential of serum miR-7, miR-16, miR-25, miR-93, miR-182, miR-376a and miR-429 in ovarian cancer patients. Br. J. Cancer *113*, 1358–1366.
12. Gallo, K.A., and Johnson, G.L. (2002). Mixed-lineage kinase control of JNK and p38 MAPK pathways. Nat. Rev. Mol. Cell Biol. *3*, 663–672.
13. Marusiak, A.A., Edwards, Z.C., Hugo, W., Trotter, E.W., Girotti, M.R., Stephenson, N.L., Kong, X., Gartside, M.G., Fawdar, S., Hudson, A., et al. (2014). Mixed lineage kinases activate MEK independently of RAF to mediate resistance to RAF inhibitors. Nat. Commun. *5*, 3901.
14. Velho, S., Oliveira, C., Paredes, J., Sousa, S., Leite, M., Matos, P., Milanezi, F., Ribeiro, A.S., Mendes, N., Licastro, D., et al. (2010). Mixed lineage kinase 3 gene mutations in mismatch repair deficient gastrointestinal tumours. Hum. Mol. Genet. *19*, 697–706.
15. Martini, M., Russo, M., Lamba, S., Vitiello, E., Crowley, E.H., Sassi, F., Romanelli, D., Frattini, M., Marchetti, A., and Bardelli, A. (2013). Mixed lineage kinase MLK4 is activated in colorectal cancers where it synergistically cooperates with activated RAS signaling in driving tumorigenesis. Cancer Res. *73*, 1912–1921.
16. Hannes, S., Abhari, B.A., and Fulda, S. (2016). Smac mimetic triggers necroptosis in pancreatic carcinoma cells when caspase activation is blocked. Cancer Lett. *380*, 31–38.
17. Luo, Q., Li, W., Zhao, T., Tian, X., Liu, Y., and Zhang, X. (2015). Role of miR-148a in cutaneous squamous cell carcinoma by repression of MAPK pathway. Arch. Biochem. Biophys. *583*, 47–54.
18. Tivnan, A., Tracey, L., Buckley, P.G., Alcock, L.C., Davidoff, A.M., and Stallings, R.L. (2011). MicroRNA-34a is a potent tumor suppressor molecule in vivo in neuroblastoma. BMC Cancer *11*, 33.
19. Zhu, W., Wang, Y., Zhang, D., Yu, X., and Leng, X. (2018). MiR-7-5p functions as a tumor suppressor by targeting SOX18 in pancreatic ductal adenocarcinoma. Biochem. Biophys. Res. Commun. *497*, 963–970.
20. Gu, D.N., Jiang, M.J., Mei, Z., Dai, J.J., Dai, C.Y., Fang, C., Huang, Q., and Tian, L. (2017). microRNA-7 impairs autophagy-derived pools of glucose to suppress pancreatic cancer progression. Cancer Lett. *400*, 69–78.
21. Bi, Y., Shen, W., Min, M., and Liu, Y. (2017). MicroRNA-7 functions as a tumor-suppressor gene by regulating ILF2 in pancreatic carcinoma. Int. J. Mol. Med. *39*, 900–906.
22. Ikeda, Y., Tanji, E., Makino, N., Kawata, S., and Furukawa, T. (2012). MicroRNAs associated with mitogen-activated protein kinase in human pancreatic cancer. Mol. Cancer Res. *10*, 259–269.
23. Akamatsu, M., Makino, N., Ikeda, Y., Matsuda, A., Ito, M., Kakizaki, Y., Saito, Y., Ishizawa, T., Kobayashi, T., Furukawa, T., and Ueno, Y. (2016). Specific MAPK-Associated MicroRNAs in Serum Differentiate Pancreatic Cancer from Autoimmune Pancreatitis. PLoS ONE *11*, e0158669.
24. Kang, H., Tan, M., Bishop, J.A., Jones, S., Sausen, M., Ha, P.K., and Agrawal, N. (2017). Whole-Exome Sequencing of Salivary Gland Mucoepidermoid Carcinoma. Clin. Cancer Res. *23*, 283–288.
25. Fawdar, S., Trotter, E.W., Li, Y., Stephenson, N.L., Hanke, F., Marusiak, A.A., Edwards, Z.C., Ientile, S., Waszkowycz, B., Miller, C.J., and Brognard, J. (2013). Targeted genetic dependency screen facilitates identification of actionable mutations in FGFR4, MAP3K9, and PAK5 in lung cancer. Proc. Natl. Acad. Sci. USA *110*, 12426–12431.
26. Slattery, M.L., Lundgreen, A., and Wolff, R.K. (2012). MAP kinase genes and colon and rectal cancer. Carcinogenesis *33*, 2398–2408.
27. Stark, M.S., Woods, S.L., Gartside, M.G., Bonazzi, V.F., Dutton-Regester, K., Aoude, L.G., Chow, D., Sereduk, C., Niemi, N.M., Tang, N., et al. (2011). Frequent somatic mutations in MAP3K5 and MAP3K9 in metastatic melanoma identified by exome sequencing. Nat. Genet. *44*, 165–169.
28. Bisson, N., Tremblay, M., Robinson, F., Kaplan, D.R., Trusko, S.P., and Moss, T. (2008). Mice lacking both mixed-lineage kinase genes Mlk1 and Mlk2 retain a wild type phenotype. Cell Cycle *7*, 909–916.
29. Ritt, D.A., Abreu-Blanco, M.T., Bindu, L., Durrant, D.E., Zhou, M., Specht, S.I., Stephen, A.G., Holderfield, M., and Morrison, D.K. (2016). Inhibition of Ras/Raf/MEK/ERK Pathway Signaling by a Stress-Induced Phospho-Regulatory Circuit. Mol. Cell *64*, 875–887.
30. Smida, M., Fece de la Cruz, F., Kerzendorfer, C., Uras, I.Z., Mair, B., Mazouzi, A., Suchankova, T., Konopka, T., Katz, A.M., Paz, K., et al. (2016). MEK inhibitors block growth of lung tumours with mutations in ataxia-telangiectasia mutated. Nat. Commun. *7*, 13701.
31. Grant, S. (2008). Cotargeting survival signaling pathways in cancer. J. Clin. Invest. *118*, 3003–3006.
32. Guo, C., and Stark, G.R. (2011). FER tyrosine kinase (FER) overexpression mediates resistance to quinacrine through EGF-dependent activation of NF-kappaB. Proc. Natl. Acad. Sci. USA *108*, 7968–7973.
33. Ma, J., Fang, B., Zeng, F., Pang, H., Zhang, J., Shi, Y., Wu, X., Cheng, L., Ma, C., Xia, J., and Wang, Z. (2014). Curcumin inhibits cell growth and invasion through up-regulation of miR-7 in pancreatic cancer cells. Toxicol. Lett. *231*, 82–91.
34. Xia, J., Cheng, L., Mei, C., Ma, J., Shi, Y., Zeng, F., Wang, Z., and Wang, Z. (2014). Genistein inhibits cell growth and invasion through regulation of miR-27a in pancreatic cancer cells. Curr. Pharm. Des. *20*, 5348–5353.
35. Ma, J., Zeng, F., Ma, C., Pang, H., Fang, B., Lian, C., Yin, B., Zhang, X., Wang, Z., and Xia, J. (2016). Synergistic reversal effect of epithelial-to-mesenchymal transition by miR-223 inhibitor and genistein in gemcitabine-resistant pancreatic cancer cells. Am. J. Cancer Res. *6*, 1384–1395.